Available online at www.sciencedirect.com
SCIENCE DIRECT®
Bioorganic & Medicinal Chemistry 13 (2005) 5797–5807
Bioorganic & Medicinal Chemistry

Branched aminoglycosides: Biochemical studies and antibacterial activity of neomycin B derivatives

Mariana Hainrichson,[a] Varvara Pokrovskaya,[a] Dalia Shallom-Shezifi,[a] Micha Fridman,[a] Valery Belakhov,[a] Dina Shachar,[b] Sima Yaron[b] and Timor Baasov[a,*]

[a]*Department of Chemistry and Institute of Catalysis Science and Technology, Technion—Israel Institute of Technology, Haifa 32000, Israel*
[b]*Department of Biotechnology and Food Engineering, Technion—Israel Institute of Technology, Haifa 32000, Israel*

Received 3 May 2005; revised 24 May 2005; accepted 25 May 2005
Available online 29 June 2005

Abstract—The C5″-OH group in neomycin B was glycosylated with a variety of mono- and di-saccharides to probe the effect of introduction of additional binding elements on antibacterial activity and interaction with the aminoglycosides modifying enzyme APH(3′)-IIIa. The designed structures show antibacterial activity superior to that of neomycin B against pathogenic and resistant strains, while in parallel they demonstrate poor substrate activity with APH(3′)-IIIa.

1. Introduction

The rapid spread of antibiotic resistance in pathogenic bacteria has prompted a continuing search for new agents capable of antibacterial activity. Indeed, microbiologists today warn of a 'medical disaster' which could lead back to the era before penicillin, when even seemingly small infections were potentially lethal. Thus, research into the design of new antibiotics is of high priority.[1–3] One way to delay the emergence of antibiotic resistance is to develop new synthetic materials that can selectively inhibit bacterial enzymes, via novel mechanisms of action. Such synthetic antibiotics are advantageous, since they have not been previously encountered by the target organism and therefore the resistance determinants are unlikely to be present in the population. However, this approach might be both time-consuming and too expensive. On the other hand, it may be less costly in time and money to employ strategies to circumvent existing bacterial resistance mechanisms and thereby to restore usefulness to antibacterials that have become compromised by resistance.[4] The remarkable advances in recent years in elucidating the mechanisms of resistance to various clinical antibiotics on the molecular level provide complementary tools to this approach via structure- and mechanism-based design.

One example of an important group of antibiotics which could benefit from such a redesign is the aminoglycosides class of antibiotics. Aminoglycosides are highly potent, broad-spectrum antibiotics with many desirable properties for the treatment of life-threatening infections.[5,6] It is believed that aminoglycosides exert their therapeutic effect by interfering with translational fidelity during protein synthesis via interaction with the A-site rRNA on the 16S domain of the ribosome.[7,8] Recent achievements in ribosome structure determination have provided fascinating new insights into the decoding site of the ribosome at high resolution and how aminoglycosides might induce misreading of the genetic code.[9–11]

Unfortunately, prolonged clinical and veterinary use of currently available aminoglycosides has resulted in effective selection of resistance to this family of antibacterial agents.[12] Currently, resistance to these agents is widespread among pathogens worldwide, which severely limits their usefulness. The primary mechanism for resistance to aminoglycosides is the bacterial acquisition of enzymes, which modify this family of antibiotics by acetyltransferase (AAC), adenyltransferase (ANT), and phosphotransferase (APH) activities. Among these enzymes families, aminoglycoside 3′-phosphotransferases [APH(3′)s], of which seven isozymes are known, are

Keywords: Aminoglycosides; Antibiotics; Antibiotic resistance; *Pseudomonas aeruginosa*.
* Corresponding author. Tel.: +972 4 829 2590; fax: +972 4 829 5703; e-mail: chtimor@techunix.technion.ac.il

0968-0896/$ - see front matter © 2005 Elsevier Ltd. All rights reserved.
doi:10.1016/j.bmc.2005.05.058

widely represented. These enzymes catalyze transfer of γ-phosphoryl group of ATP to the 3′-hydroxyl of many aminoglycosides, rendering them inactive because the resulted phosphorylated antibiotics no longer bind to the bacterial ribosome with high affinity. Due to the unusually broad spectrum of aminoglycosides that can be detoxified by APH(3′) enzymes, much effort has been put into understanding the structural basis for their promiscuity in substrate recognition and catalysis.[13]

To tackle the problem of resistance, many structural analogs of natural aminoglycosides have been synthesized over the past decade. In the majority of these studies a minimal structural motif, the neamine moiety (rings I and II of neomycin B, Fig. 1), which is common for a series of structurally related aminoglycosides, has been identified and used as a scaffold for the construction of diverse analogs as potential new antibiotics.[14] Some of the designed structures showed considerable antibacterial activities.

Unlike this strategy, we have recently hypothesized that since aminoglycoside antibiotics exert their antibacterial activity by selectively recognizing and binding to rRNA, it is likely that by maintaining the backbone of selected antibiotic but adding additional recognition/binding elements, improved binding to rRNA and probably better antibacterial performance are expected to result. Using this strategy, in combination with the reported structural details on the interaction of neomycin B (NeoB) with APH(3′) enzyme and with the A-site bacterial ribosome, we have previously reported our preliminary results on the synthesis and antibacterial activity of the first generation of pseudo-pentasaccharide derivatives of NeoB (structures **4**, **5**, **7**, and **8**).[15] Encouraged by the observed antibacterial activity of these structures, which were superior to that of NeoB against selected bacterial strains, we designed seven more derivatives (structures **1**–**3**, **6**, **9**–**11**, Fig. 1). Recently, these compounds were shown to be potential anti-anthrax drugs, having a dual effect by inhibiting the anthrax lethal factor toxin and at the same time also displaying anti *Bacillus anthracis* activity.[16] In the current study, the antibacterial activities of all new structures against various pathogenic and resistant bacterial strains, along with kinetic studies of **1**–**11** with the aminoglycoside-modifying enzyme APH(3′)-IIIa, are reported.

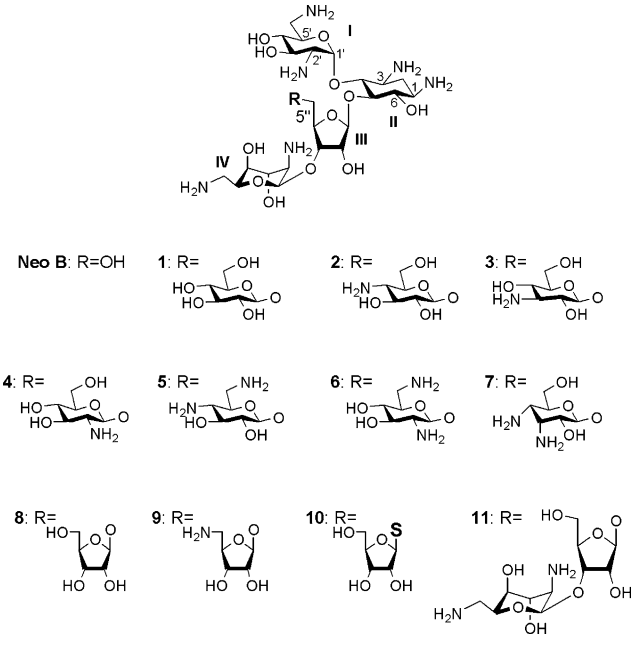

Figure 1. Structures of neomycin B (NeoB) and the synthetic analogs **1**–**11**.

2. Results and discussion

2.1. Design strategy of branched aminoglycosides

The X-ray structures of the aminoglycoside kinase APH(3′)-IIIa ternary complex with NeoB and ADP,[13] and that of paromomycin I (contains C6′-OH instead of C6′-NH_2 in NeoB) bound to A-site bacterial ribosome[9] were employed for our design. Superposition of these two structures revealed that all the functional groups of aminoglycosides that are utilized for rRNA binding are identical in both complexes, with the exception of two, which are not employed for binding in the antibiotic-resistant enzyme.[13] One of these groups is the C5″-OH of NeoB which is phased toward the second substrate, ATP, and may have crucial role for the formation of the reactive ternary complex prior the phosphorylation step. Previous studies suggested that in the presence of APH(3′)-IIIa, NeoB undergoes phosphorylation on two distinct positions: the C3′-OH and the C5″-OH. Further more, it has been reported that 77% of the initial phosphorylation takes place on the C5″-OH position.[17] Based on these data, we anticipated that incorporation of gross changes, such as addition of an extra rigid sugar ring at C5″-OH, in addition to disabling the APH(3′)-IIIa from phosphorylating the initially preferred C5″-OH may also cause a dramatic effect on the formation of a precise ternary complex required for the phosphorylation of the C3′-OH. In addition, if the added sugar contains potential functionalities directed for the recognition/binding to RNA, superior binding to rRNA is expected. Indeed, enhanced RNA binding by using dimerized aminoglycosides and various bifunctional aminoglycosides supported this hypothesis.[18,19]

Taken together with the relative ease of derivation of a primary alcohol, we selected position C5″ in NeoB as a modification site and prepared a series of branched derivatives **1**–**11**. These structures keep the whole antibiotic constitution intact as a recognition element to the rRNA, while the extended sugar ring(s) (ring V in structures **1**–**10**, and rings V and VI in **11**) of each structure was designed in a manner that incorporates either *cis*-1,2-diamine (**7**), flexible 1,3-diamine (**5**), *cis*-1,3-hydroxyamine (**2**, **4**–**6**), or ribofuranose ring (**8**–**10**) as potential functionalities directed for the recognition of the phosphodiester bond of RNA.[20–22] The design of the new structures **1**–**3**, **6**, **9**–**11** was based on the results obtained from the first generation structures **4**, **5**, **7**, **8**.[15] Thus, since **8** was found to be as potent as NeoB against

both Gram-negative and Gram-positive bacterial strains, we further modified it and prepared structures **9** and **10**, with the expectation that the addition of extra positive charge in **9** may increase binding affinity to RNA,[23] and the replacement of the glycosidic bond between rings III and V to the thioglycoside in **10** could increase its acid stability and/or in vivo stability against the action of various glycosidase enzymes. With the structures **1**–**3** and **6**, we aimed to get more insight about the structure–activity relationship on the additional glucopyranose ring (ring V).

2.2. Antibacterial activity

Antibacterial activities of the new analogs were determined by measuring the minimal inhibitory concentrations (MICs) against both Gram-negative and Gram-positive bacteria, including pathogenic and resistant strains, using the microdilution assay (Table 1). Resistant strains included *Escherichia coli* XL1(pET9d), *Salmonella enterica serotype virchow* (SV49), and *Pseudomonas aeruginosa* (ATCC 27853). *E. coli* XL1(pET9d) is an antibiotic-sensitive laboratory strain that harbors plasmid pET9d with the cloned aminoglycoside kinase APH(3′)-Ia (Novagen Inc.). *S. virchow* (SV49) is a multidrug-resistant strain obtained from poultry and found to be resistant to streptomycin, tetracycline, ampicillin, sulfa, kanamycin, and NeoB (S. Yaron, unpublished data). The mechanism(s) of resistance of this strain is still under investigation. *P. aeruginosa* strains possess several different resistance mechanisms to aminoglycosides, including the chromosomal encoded APH(3′)-IIb enzyme,[24] and the multidrug efflux system MexXY.[25–27]

As described previously, compound **8**, the derivative in which plain ribose was added to the C5″-OH of NeoB, displayed antibacterial activities similar to those of NeoB and kanamycin A (KanA) against most of the bacterial strains tested, and showed somewhat better activity against the pathogenic multiresistant *S. virchow*.[15] Surprisingly, when the glycosidic bond between the new ribose (ring V) and ring III of NeoB was replaced by thio-glycosidic bond in **10**, the antibacterial activity against most strains was significantly hampered. Similarly, replacement of the primary hydroxyl of ring V with amine in **9**, also resulted in reduced antibacterial effect, against most bacterial strains, with the exception of *P. aeruginosa*, as described below.

P. aeruginosa is a pathogenic bacterium which is a major cause of mortality among cystic fibrosis patients.[28,29] One of the efficient treatments offered in cases of *P. aeruginosa* respiratory system infections is based upon aerosol inhalation therapy of aminoglycosides.[30,31] Unfortunately, in recent years, increasing numbers of *P. aeruginosa* clinical isolates were found to be resistant to several antibiotics, preventing effective treatment. As seen in Table 1, the growth of *P. aeruginosa* (ATCC 27853) was inhibited by several of the new derivatives. Compounds **2**, **4**, **8**, **9**, and **11** showed similar MIC values to that of NeoB, while compounds **5** and **6** where better than NeoB, as further demonstrated by the larger inhibition radius caused by these derivatives (Fig. 2). The observed better activity could be a result of better influx, improved binding of these compounds to the bacterial rRNA, reduced susceptibility to aminoglycoside-modifying enzymes, reduced extraction by the efflux pumps, or a combination of several of these mechanisms.

Careful inspection of the MIC values against *P. aeruginosa* presented in Table 1 reveals an interesting structure–activity relationship. The antibacterial activity of the glucopyranose based analogues (having a glucose substituent at ring V, compounds **1**–**6**) increases gradually with the increasing number of amino groups on the ring: $(2NH_2)$glucose (**5**, **6**) > $(1NH_2)$glucose (**2**, **3**, **4**) > glucose (**1**). In this series of compounds, no particular influence on the position of the amino group(s) on the glucose ring is observed. In the ribose-based derivatives **8** and **9**, the addition of an amine has also improved the

Table 1. Minimal inhibitory concentration (MIC) values of KanA, NeoB and **1**–**11** against various bacterial strains

Compound	MIC (μg/mL)[a]						
	E. coli (R47-100)	*E. coli* (ATCC 25922)	*E. coli* XL1 blue/pET9d	*Staphylococcus epidermidis* (ATCC 12228)	*Bacillus subtilis* (ATCC 6633)	*Salmonella virchow* (SV49)	*Pseudomonas aeruginosa* (ATCC 27853)
KanA	ND[b]	ND	256	ND	ND	512	512
NeoB	8	10	64	0.5	1	256	64
1	128	128	>512	5	10	>512	>512
2	64	64	320	8	8	>1024	**40**
3	80	80	>640	2	2	1024	128
4	40	32	>256	2	2	>1024	**40**
5	64	64	>256	2	4	>1024	**32**
6	80	64	256	8	8	>1024	**32**
7	80	128	>256	8	10	>1024	128
8	**8**	**10**	**64**	**0.5**	**1**	**128**	**64**
9	64	64	320	8	8	>1024	**40**
10	128	160	>640	16	10	>512	512
11	256	160	512	5	10	>1028	**64**

[a] The MIC values represent the results obtained in parallel experiments with two different starting concentrations of the tested compound (640 and 1024 μg/mL).

[b] ND refers not determined. MIC values of the designed structures, which are similar or lower to that of NeoB are in bold.

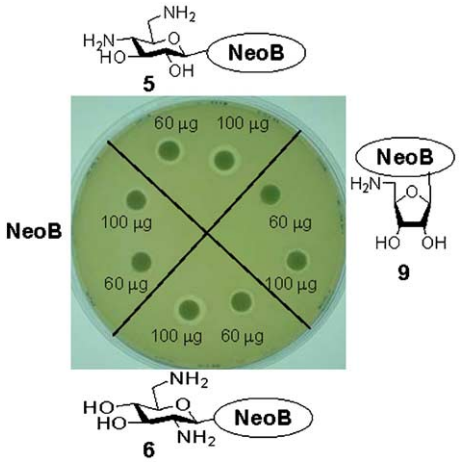

Figure 2. Kirby-Bauer disk assay illustrating *P. aeruginosa* (ATCC 27853) growth inhibition by NeoB and the derivatives **5**, **6**, and **9**. Paper disks containing known amounts of antibiotic (60 and 100 μg/disk) are placed on plates inoculated with bacterial culture, and the diameters of the zones of inhibition, apparent as clear regions around the disks, are measured after overnight growth.

activity against *P. aeruginosa*. However, the presence of a diamino sugar itself is not enough for good anti-*P. aeruginosa* activity, as seen from the high MIC value of the diamino-D-allose derivative **7**. This analog differs from the gluco-based derivatives in the configuration at the C3 position, suggesting that the unusual *cis*-1,2-diamine substitution at ring V of this analog damages the antibacterial activity.

The observation that the new derivatives affect differently the various bacteria tested could be explained mainly by the diverse resistance mechanisms displayed by these strains, and/or by their different permeability to the compounds. To determine whether the new modifications in compounds **1**–**11** indeed resulted in decreased phosphorylation by an APH(3′) resistance enzyme, we used two complementary approaches. We tested the ability of compounds **1**–**11** to serve substrates of purified APH(3′)-IIIa (described below), and determined the MIC values of selected compounds against two isogenic *E. coli* strains (Table 2). *E. coli* BL21(DE3) is a non-resistant strain, and its transformation with the pET-SACG1 plasmid (which contains the APH(3′)-IIIa gene) makes it resistant to NeoB and KanA.[32] Since the aminoglycoside resistance of the latter is mediated only by the presence of the cloned APH(3′)-IIIa, comparison of the MIC values against these two strains eliminates other effects that could reduce the activity of the different molecules, like solubility or penetration. Consequently, low ratio between the MIC values of the resistant and non-resistant strains should suggest that the compound is a poorer substrate for the resistance enzyme.

As seen from the data in Table 2, when the APH(3′)-IIIa enzyme is expressed in the cell, the MIC values for KanA and NeoB are raised by 51- and 16-fold, respectively. Interestingly, all of the new compounds tested were less effective against the non-resistant strain compared to KanA and NeoB, with MIC values in the range of 30–80 μg/mL, suggesting reduced binding of these derivatives to the bacterial ribosome, or alternatively, their lower penetration through the bacterial membrane. Against the resistance-carrying strain, however, most of the compounds displayed similar or better antibacterial activities to that of KanA, and lower activity than that of NeoB. As such, the ratios between the MIC values of the resistant and non-resistant strains for all new derivatives tested, were lower than that of NeoB, indicating that the new compounds are poorer substrates of APH(3′)-IIIa than NeoB. To substantiate this observation, the detailed kinetic analysis of the purified APH(3′)-IIIa with new derivatives was carried out.

Table 2. MIC values of KanA, NeoB, and several of the new derivatives against *E. coli* BL21(DE3) (background strain) and its engineered variant BL21(DE3)/pETSACG1 expressing APH(3′)-IIIa

Compound	MIC (μg/mL)[a]		
	BL21(DE3)	BL21(DE3)/pETSACG1	Ratio[b]
KanA	10	512	51
NeoB	10	160	16
1	64	640	10
2	80	512	6.4
5	80	512	6.4
6	40	256	6.4
8	32	320	10
9	64	512	8

[a] The MIC values represent the results obtained in parallel experiments with two different starting concentrations of the tested compound (640 and 1024 μg/mL).

[b] The ratio was calculated by dividing the MIC value against BL21(DE3)/pETSACG1 to that against BL21(DE3).

2.3. Kinetic analysis

The catalytic activity of APH(3′)-IIIa with compounds **1**–**11** was studied using the pyruvate kinase–lactate dehydrogenase coupled assay system (Table 3). The kinetic constants measured for KanA and NeoB were similar to previously reported values.[32] The observed data indicate that all new derivatives are poorer substrates of APH(3′)-IIIa than NeoB. The K_m values of all of the designed compounds were 2- to 5-fold higher than those of NeoB and KanA, with the exception of

Table 3. Kinetic parameters for the phosphorylation of KanA, NeoB, and **1**–**11** by APH(3′)-IIIa

Compound	K_m (μM)	k_{cat} (s^{-1})	$(k_{cat}/K_m)/10^4$ ($M^{-1}s^{-1}$)
KanA	11.6 ± 0.4	1.6 ± 0.1	14
NeoB	8.8 ± 0.5	2.5 ± 0.1	28
1	31 ± 2.3	2.6 ± 0.1	8.3
2	45 ± 3.3	2.4 ± 0.1	5.1
3	35 ± 4.0	3.4 ± 0.1	9.7
4	31 ± 2.9	4.0 ± 0.1	12
5	39 ± 4.4	1.0 ± 0.1	2.5
6	50 ± 3.0	3.4 ± 0.1	6.7
7	24 ± 1.9	2.9 ± 0.1	12
8	29 ± 2.5	1.6 ± 0.1	5.4
9	51 ± 6.0	1.5 ± 0.1	3.0
10	12.7 ± 0.9	1.6 ± 0.1	13
11	46 ± 4.2	3.1 ± 0.2	6.7

compound **10** which had K_m only slightly higher than that of NeoB. For all of the tested compounds, the k_{cat} values varied between 1 and 4 s^{-1}, similar to those of NeoB and KanA. As a result, the specificity constant values (k_{cat}/K_m) of **1**–**11** were lower than that of NeoB. Compounds **5** and **9** displayed the lowest specificity constants, of about 10-fold lower than that of NeoB, implying that these derivatives are the least phosphorylated by APH(3′)-IIIa. Interestingly, **5** and **9** displayed particularly good activity against *P. aeruginosa*, which harbors a chromosomal APH(3′)-IIb-encoding gene (Table 1). Thus, although to date no detailed kinetic and biochemical studies of the APH(3′)-IIb are available, these observations suggest that the two resistant enzymes APH(3′)-IIIa and APH(3′)-IIb may share similar substrate preferences.

The combined kinetic (Table 3) and antibacterial activity (Table 2) data demonstrate that the new derivatives are indeed poorer substrates than the parent NeoB for the resistance determinant APH(3′) enzyme, while in parallel they keep significant antibacterial activities. However, according to the kinetic analysis of **1**–**11** described above, these compounds are still being phosphorylated by APH(3′)-IIIa in spite of the blockage introduced at the C5″-OH position. To estimate possible positions in derivatives **1**–**11** that might be phosphorylated by APH(3′)-IIIa, molecular docking experiments were performed, and representative results for compounds **2** and **8** are discussed.

2.4. Molecular docking

Several three-dimensional crystal structures of APH(3′)-IIIa were previously determined: of an apo-protein, of complexes with ADP or 5′-adenylylimidodiphosphate (AMP-PNP) which is a non-hydrolyzable ATP analog, and of two ternary complexes with ADP and either KanA, or NeoB.[13,33,34] For the docking experiments, we used the protein scaffold from the APH(3′)-IIIa · ADP · KanA complex, into which the structure of ATP was modeled based on the structures of the ADP and AMP-PNP (see Section 4 for details).

Flexible docking of **2** and **8** into the APH(3′)-IIIa · ATP modeled structure was performed. For each of the molecules, 20 poses with the highest docking scores were examined, and their likelihood to represent a possible productive catalytic conformation was evaluated using the distances of hydroxyl groups to the ATP γ-phosphoryl and to the general base residue Asp190. In most poses with the highest scores, rings I–III were found in similar positions to the corresponding rings in the crystal structure of NeoB, such that the C3′-OH is closest to the ATP γ-phosphoryl and to Asp190 (two such examples are shown in Fig. 3). In both **2** and **8** models, ring IV is located deeper in the active site pocket compared to its location in the NeoB structure, facilitating the binding of the new ring (ring V). Thus, these results show that the introduction of the additional rings at the C5″ position have not perturbed the binding of the neamine parts of these molecules into the APH(3′)-IIIa active site, and therefore the new derivatives can still be phosphorylated at the C3′-OH position.

Almost no poses in which other hydroxyls, except C3′-OH, of either **2** or **8** are located in an appropriate position for phosphorylation were obtained. It should be noted, however, that this result does not suggest that such conformations are not possible. Indeed, when flexible docking experiments of the NeoB molecule into the APH(3′)-IIIa · ATP modeled structure were performed (data not shown), no poses in which the C5″-OH was in an appropriate position for phosphorylation were obtained. It appears therefore that the specific active site structure in which the APH(3′)-IIIa is trapped in this crystal structure prompts the binding of NeoB in the orientation that allows the C3′-OH phosphorylation and not the C5″-OH phosphorylation. It seems that for a C5″-OH phosphorylation, both the enzyme and the NeoB molecules would need to adopt different conformations than those of the C3′-OH phosphorylation.

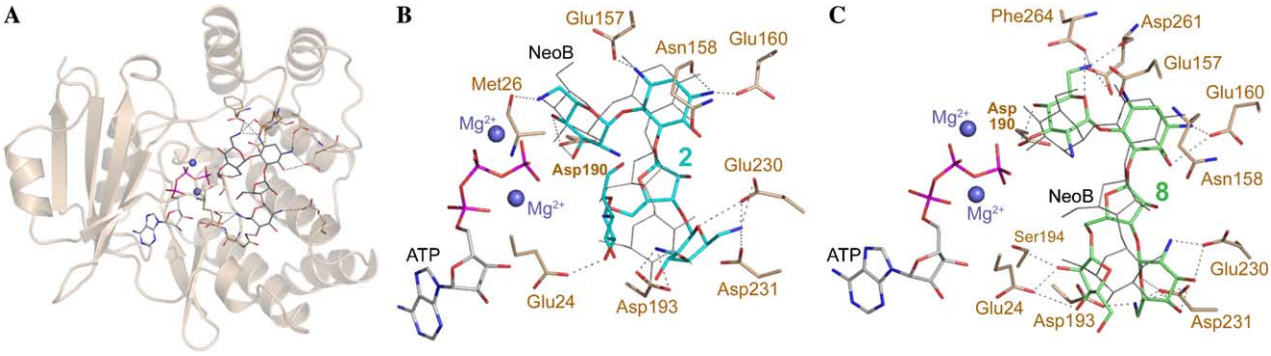

Figure 3. Docking of compounds **2** and **8** into the active site of APH(3′)-IIIa. (A) The overall APH(3′)-IIIa structure in complex with ATP, two Mg^{2+} ions, and the NeoB molecule. The original structure contained an ADP molecule (PDB accession number 1L8U), was converted to ATP based on the structure of the enzyme in complex with AMP-PNP (PDB accession number 1J7U), as described in Section 4. This structure (without the NeoB molecule) was used as a template for the docking experiments. Oxygens are in red, nitrogens are in blue, phosphates are in pink, Mg^{2+} ions are in purple, carbon atoms of the protein residues are in brown, and carbon atoms of ATP and NeoB are in gray. (B) The docked conformation of **2** into the active site with the carbon atoms in cyan. The original crystal structure position of NeoB is also shown (gray lines). Potential hydrogen bonds between **2** and the protein are shown as dotted lines. (C) The docked conformation of **8** inside the active site with the carbon atoms in green. The original crystal structure position of NeoB is also shown (gray lines). Potential hydrogen bonds between **8** and the protein are shown as dotted lines.

Since the docking experiments of the new derivatives was done on the crystal structure in which NeoB is C3′-OH phosphorylated, it is not surprising that the resulting poses are also those in which only the C3′-OH of these compounds is phosphorylated.

Nevertheless, while the docking experiments predicted the possibility of phosphorylation at C3′-OH, the question of whether the C3′-OH is the only position at which the new derivatives are phosphorylated or they have multiple phosphorylation sites, remains an open question. In attempts to answer this question and also to verify the molecular docking data, substrate activities of new derivatives were subjected to ^{31}P NMR assay.

2.5. Monitoring of APH(3′)-IIIa activity by ^{31}P NMR

Using HPLC, it was previously shown that in NeoB there are two possible positions that are phosphorylated by APH(3′)-IIIa, the C5″-OH and the C3′-OH. In 77% of the molecules, the first phosphoryl-transfer occurs on the C5″-OH position, and these C5″-*O*-phosphorylated molecules can be further phosphorylated on the C3′-OH.[17] To test the feasibility of the ^{31}P NMR assay for monitoring APH(3′)-IIIa-catalyzed reactions, initially the experiments were performed on the NeoB as a standard. The ^{1}H-coupled (Fig. 4A) and ^{1}H-decoupled (Fig. 4B) ^{31}P NMR spectra of NeoB after 6 h incubation with the APH(3′)-IIIa show three distinct peaks in the region of 1.5–2.4 ppm. The two doublets centered at 2.11 and 1.96 ppm were assigned as secondary 3′-phosphates of diphosphorylated and monophosphorylated NeoB, respectively. The peak at 1.66 ppm with the multiplicity of triplet, and the same integrated area as the peak at 2.11 ppm, corresponds to the 5″-phosphate of the diphosphorylated NeoB. The time course of this reaction (data not shown) clearly showed that as the reaction starts two monophosphorylated derivatives of NeoB, 3′-phosphate and 5″-phosphate are initially formed. As the reaction progresses, second phosphorylation of the 5″-phosphate is much faster than that of the 3′-phosphate to generate the 3′,5″-diphosphate. Thus, after 6 h two main derivatives of Neo B, 3′-phosphate and 3′,5″-diphosphate, were detected in accordance with previous reports.[17]

The same experiment with compound **2** clearly showed that in this derivative, similarly to NeoB, there are at least two distinct positions that undergo enzyme-catalyzed phosphorylation (Fig. 5). As the phosphorylation of **2** progresses, the peaks of ATP phosphates are gradually decrease with the subsequent increase of ADP phosphates. The two peaks centered at 1.91 and 1.74 ppm, corresponding to phosphates of the phosphorylated **2**, appear simultaneously and grow at the same rate. ^{1}H-coupled ^{31}P NMR spectrum of this area after 360 min incubation (Fig. 5, inset A) shows a doublet (1.91 ppm) and triplet (1.74 ppm) indicative of phosphates on secondary and primary hydroxyl, respectively. Since the only primary hydroxyl in this molecule

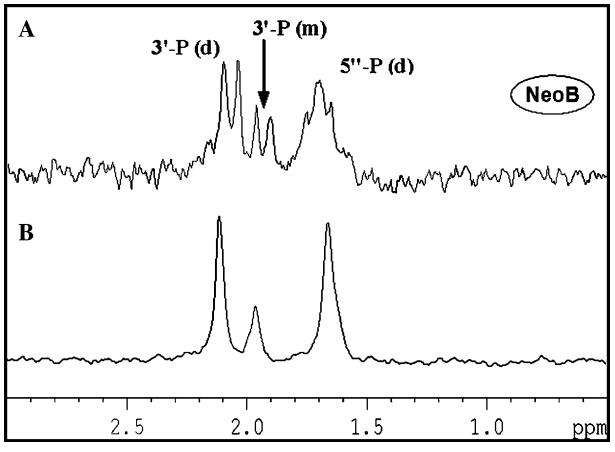

Figure 4. ^{1}H-coupled (A) and ^{1}H-decoupled (B) ^{31}P NMR spectra of NeoB (44 mM) recorded after a 6 h incubation at 37 °C in the presence of Tris–HCl buffer (50 mM), pD 7.1, KCl (40 mM), $MgCl_2$ (10 mM), ATP (132 mM) and APH(3′)-IIIa (150 μL, 0.72 U/mL stock solution) in a total volume of 0.65 mL D_2O. 3′-P (d) and 5″-P (d) refer to the 3′-phosphate and 5″-phosphate, respectively, in the 3′,5″-diphospho-NeoB. 3′-P (m) refers to the 3′-phosphate of 3′-phospho-NeoB.

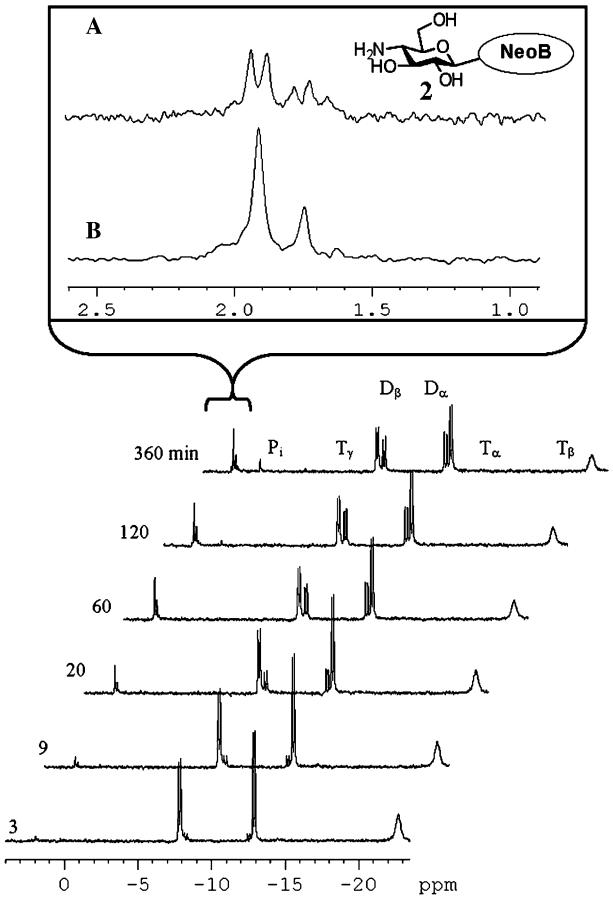

Figure 5. A time course of ^{1}H-decoupled ^{31}P NMR spectra showing the phosphorylation of **2** (44 mM) at 37 °C in the presence of Tris–HCl buffer (50 mM), pD 7.1, KCl (40 mM), $MgCl_2$ (10 mM), ATP (132 mM), APH(3′)-IIIa (150 μL, 0.72 U/mL stock solution) in a total volume of 0.65 mL D_2O. T_α, T_β, and T_γ refer to the α-, β-, and γ-phosphates of ATP, respectively. D_α, and D_β refer to the α-, and β-phosphates of ADP, respectively. P_i refers to inorganic phosphate. The inset shows enlarged regions of the ^{1}H-coupled (A) and the ^{1}H-decoupled (B) ^{31}P NMR spectra of the phosphorylated **2** after 360 min.

is located on the ring V (C6-OH), it appears that the enzyme is capable of phosphorylating the newly introduced sugar as well. The second phosphorylation, on a secondary hydroxyl, is probably on the C3′-OH, similarly to the NeoB.

Interestingly, when the same reaction was performed with compound **8**, in addition to the phosphorylation of a secondary hydroxyl, a peak indicative of the phosphorylation of a primary hydroxyl, most probably the primary hydroxyl of the additional ribose ring (ring V), was also observed (data not shown). However, similar experiments with other derivatives that lack primary hydroxyl also showed multiple phosphorylations, implying that in this set of new derivatives the primary hydroxyl of ring V is not the only site that undergoes additional phosphorylation. This can be clearly seen from the time-course experiment of compound **6**, which is shown in Figure 6 as the representative example. The two peaks centered at 1.55 and 1.75 ppm appear and grow at the same rate, while the third peak at 2.05 ppm evolves only after about 60 min of incubation

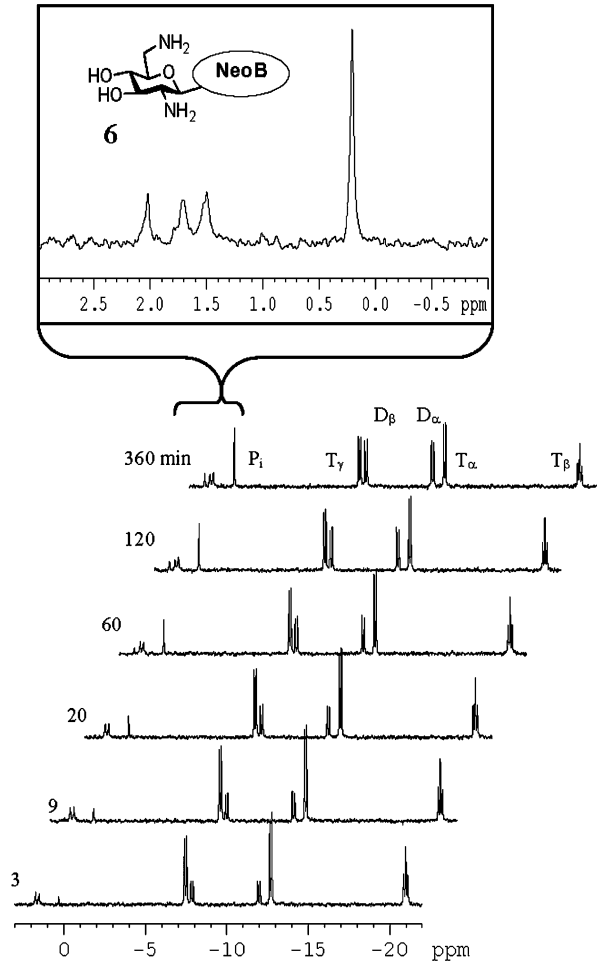

Figure 6. A time-course of ^{1}H-decoupled ^{31}P NMR spectra showing the phosphorylation of **6** (44 mM) by APH(3′)-IIIa. The reaction conditions were exactly the same as outlined in the legend of Figure 5. The inset shows enlarged region of the phosphorylated **6** and of the P_i after 360 min.

and after 360 min it reaches the same intensity as the previous two.

Thus, although at this stage we did not attempt to give the exact assignment of each single peak in ^{31}P NMR spectra, from the current data it is clear that the blockage of C5″-OH in **1**–**11** has not prevented the binding of new derivatives into the enzyme active site, nor does it eliminate the ability of APH(3′)-IIIa to perform multiple phosphorylations. This suggests that several different conformations of the designed structures can bind productively into the APH(3′)-IIIa active site and lead to the enzyme-catalyzed phosphoryl transfer process. Some of these conformations might be unproductive for the phosphoryl transfer, but they can facilitate side reactions such as adverse ATPase activity of the enzyme. Indeed, while the ^{31}P NMR experiment with compound **2** (as well as the experiments with the NeoB and compound **8**) showed only marginal formation of inorganic phosphate (P_i, Fig. 5), the same experiment with compound **6** resulted considerably high ATPase activity at any time of the reaction progress and reached about 50% of the total enzyme activity at 60 min of incubation (Fig. 6). Such an elevated ATPase activity of APH(3′)-IIIa with compound **6** could also explain its somewhat higher turnover number for **6** (k_{cat} = 3.4 s^{-1}, Table 3) to that for compound **2** (k_{cat} = 2.4 s^{-1}).

3. Summary and conclusions

In this study, we have attempted to probe the effect of introduction of additional binding elements in aminoglycoside antibiotic on antibacterial activity and interaction with the aminoglycosides modifying enzyme APH(3′)-IIIa. For this purpose we have generated a new class of branched aminoglycosides (**1**–**11**) by linking a variety of sugar substituents at the C5″-OH group of the clinically important antibiotic NeoB, and the resulted structures were examined against various bacterial strains including pathogenic and resistant strains. While several of the designed structures exhibited activities similar to or better than that of the parent NeoB against selected strains, the observed excellent activities of the majority of the derivatives against *P. aeruginosa* were particularly important. In this case, a remarkable structure–activity relationship of the glucopyranose based analogs (compounds **1**–**6**) was observed, so that the antibacterial activity increases gradually with the increasing number of amino groups on the additional glucose ring (ring V): ($2NH_2$)glucose (**5**, **6**) > ($1NH_2$)glucose (**2**, **3**, **4**) > glucose (**1**). The detailed kinetic analysis with the purified APH(3′)-IIIa enzyme, along with the biological activities tested against two isogenic *E. coli* strains, one with harbored APH(3′)-IIIa and second the background strain without the resistant enzyme, revealed that the new derivatives are indeed inferior substrates for the APH(3′)-IIIa compared to NeoB. Based on these data it is suggested that the particularly good antibacterial activities of the designed structures against *P. aeruginosa* may involve their reduced substrate activities to the APH(3′)-IIb resistance enzyme, the gene of which is chromosomally encoded in *Pseudomonas*.

4. Experimental

4.1. General techniques

^{1}H NMR, ^{13}C NMR, DEPT, COSY, 1D TOCSY, HMQC, spectra were recorded on a Bruker Avance™ 500 spectrometer. Chemical shifts reported (in parts per million) are relative to internal Me_4Si ($\delta = 0.0$) with $CDCl_3$ as the solvent, and to HOD ($\delta = 4.63$) with D_2O as the solvent. Mass spectral analysis were performed on a Bruker Daltonix Apex 3 mass spectrometer under electron spray ionization (ESI), TSQ-70B mass spectrometer (Finnigan Mat) or under MALDI-TOF on an α-cyano-4-hydroxycinnamic acid matrix on a MALDI Micromass spectrometer. Reactions were monitored by TLC on Silica gel Gel 60 F_{254} (0.25 mm, Merck), and spots were visualized by charring with a yellow solution containing $(NH_4)_6Mo_7O_{24}{\cdot}4H_2O$ (120 g) and $(NH_4)_2Ce(NO_3)_6$ (5 g) in 10% H_2SO_4 (800 mL). Flash column chromatography was performed on Silica gel Gel 60 (70–230 mesh). All reactions were carried out under an argon atmosphere with anhydrous solvents, unless otherwise noted. All chemicals, unless otherwise stated, were obtained from commercial sources.

4.2. Synthetic part

The synthesis of compounds **1**, **2**, **4**–**11** was described previously.[15,16] Compounds **12**[35] and **15**[15] were prepared as previously reported. The 3-amino-glucopyranoside derivative of NeoB, compound **3**, was prepared by NIS-promoted coupling of the neomycin acceptor **15** with the thioglycoside donor **14** followed by a standard two step deprotection: removal of all the ester groups by treatment with methylamine (33% solution in EtOH) and reduction of all the azido groups by the Saudinger reaction, as outlined in Scheme 1. The formation of all the intermediate (**12**–**16**) and the final (**3**) structures were confirmed by a combination of various spectroscopic techniques, including HMQC, HMBC, 2D COSY, and 1D TOCSY NMR spectroscopy, as outlined below.

4.2.1. *p*-Methylphenyl-3-deoxy-3-azido-2,4,6-tri-*O*-benzoyl-1-thio-D-glucopyranoside (14). The title compound was prepared from the readily available **12**[35] by the following steps.

To a mixture of **12** (2.45 g, 8.58 mmol) in dioxane (5 mL), 2 N solution of HCl (5 mL), was added. Propagation of the reaction was monitored by TLC (MeOH 20%, dichloromethane 80%). After 1 h the pH was adjusted to ~7 by $NaHCO_3$ (satd). The reaction mixture was filtered, the filtrate was washed with MeOH, and the combined organic fraction was evaporated to afford the crude product (1.76 g).

The crude from the previous step was dissolved in pyridine (20 mL), and a catalytic amount of 4-DMAP and acetic anhydride (6.5 mL, 68.75 mmol), were added. After about 2 h the mixture was diluted with EtOAc and neutralized with $NaHCO_3$ (satd). The organic layer was dried over $MgSO_4$, evaporated, and purified by column chromatography (silica gel, EtOAc/hexane) to yield the corresponding tetra-acetate as a white solid (3.0 g, 94%). ^{1}H NMR (300 MHz, $CDCl_3$) δ: 2.07–2.02 (m, OCO*Me*), 3.61 (dd, $J_1 = J_2 = 10.2$ Hz, H-3), 3.75–3.68 (m, H-5), 4.12–3.98 (m, H-6, H-6′), 5.00–4.93 (m, H-2, H-4), 6.24 (d, $J = 3.6$ Hz, H-1). ^{13}C NMR (125 MHz, $CDCl_3$) δ: 20.8, 20.9, 21.0, 21.1, 64.5, 68.0, 70.2, 73.9, 89.0, 92.2 (C-1), 168.9, 169.2, 169.4, 169.7, 171.0. ESI-MS *m*/*z* 396.1 ($M+Na^+$, $C_{14}H_{19}N_3O_9$ requires 396.3).

To a mixture of the tetra-acetate from the previous step (3.0 g, 8.04 mmol) and *p*-thiocresol (1.25 g, 0.01 mol) in CH_2Cl_2 (50 mL) boron trifluoride diethyl etherate (3 mL, 0.023 mol) was added. The mixture was stirred overnight and then diluted with CH_2Cl_2 (200 mL) and washed with saturated $NaHCO_3$ (120 mL) and water

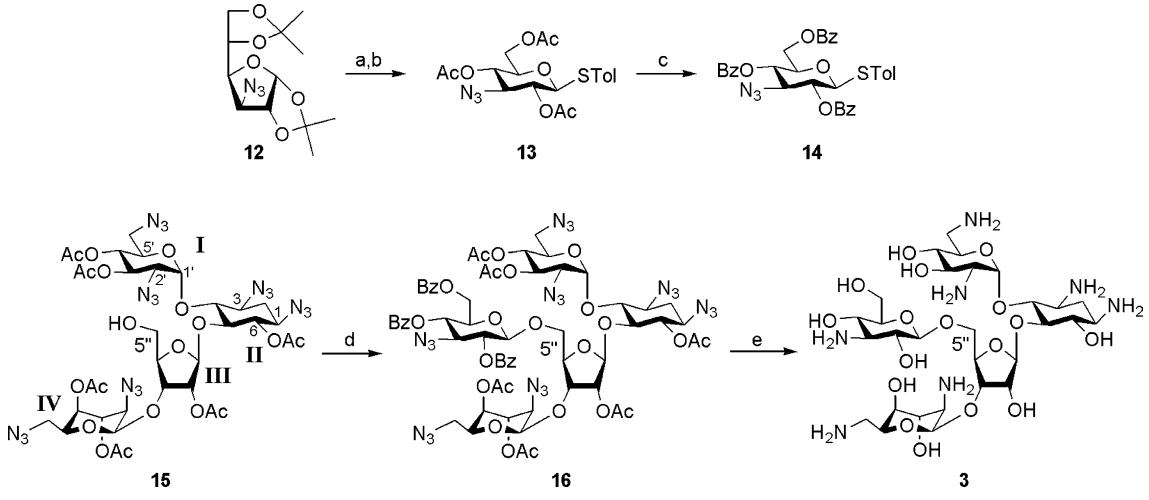

Scheme 1. General synthetic pathways for the assembly of compound **3**. Reagents and conditions: (a) i—2 N HCl, dioxane, room temperature; ii—Ac_2O, pyridine, DMAP (cat.), room temperature, 94%; (b) TolSH (1.2 equiv), $BF_3{\cdot}Et_2O$ (3 equiv), CH_2Cl_2, room temperature, 34.3%; (c) i—NaOMe (0.5 M in MeOH) (cat.), MeOH/CH_2Cl_2 (2:1); ii–BzCl (3.5 equiv), DMAP (cat.), pyridine, ambient temperature, 97%; (d) **14**, NIS, TfOH, CH_2Cl_2, −40 °C, 57%; (e) i—$MeNH_2$ (33% in EtOH), ii—PMe_3, NaOH (0.1 M), THF/H_2O (3:1), 81%. Bz = benzoyl, Tol = tolyl, DMAP = 4-dimethyl aminopyridine, NIS = *N*-iodosuccinimide, Tf = trifluoromethanesulfonyl.

(100 mL). The organic layer was dried over Na_2SO_4. The solvent was removed, and the residue was purified by column chromatography on silica gel (hexane/EtOAc 3:1) to give **13** (1.2 g, 34.3%) as a syrup. ^{1}H NMR (300 MHz, $CDCl_3$) δ: 2.02 (s, 3H, OCO*Me*), 2.05 (s, 3H, OCO*Me*), 2.12 (s, 3H, OCO*Me*), 2.29 (s, 3H, *Me*S-Tol), 3.61–3.55 (m, 2H, H-3, H-5), 4.11–4.10 (dd, 2H, H-6, H-6′), 4.52 (d, 1H, J = 9.9 Hz, H-1), 4.85–4.78 (m, 2H, H-2, H-4), 7.06 (d, 2H, J = 8.4 Hz, *ortho* to the methyl of STol), 7.33 (d, 2H, J = 8.4 Hz, *ortho* to the sulfur of STol). ^{13}C NMR (125 MHz, $CDCl_3$) δ: 22.4, 22.6, 22.7, 23.0, 64.0, 67.6, 70.1, 71.8, 78.1, 88.2 (C-1), 131.5, 135.4. ESIMS *m*/*z* 460.1 (M+Na^+, $C_{19}H_{23}N_3O_7S$ requires 460.5).

To a suspension of **13** (1.2 g, 2.74 mmol) in dry MeOH (20 mL) and dry dichloromethane (10 mL), catalytic amount of NaOMe (0.5 M solution in MeOH) was added at 0 °C. Propagation of the reaction was monitored by TLC (MeOH 10%, dichloromethane 90%). After 2 h the reaction mixture was neutralized by Dowex H^+ and evaporated to dryness. The residue was dissolved in dry pyridine (20 mL) under argon and added with a catalytic amount of DMAP. After being stirred at ambient temperature for 5 min, benzoyl chloride (1.1 mL, 9.45 mmol) was added to the reaction mixture. Propagation of the reaction was monitored by TLC (EtOAc 30%, hexane 70%), which indicated completion after 4 h. The reaction mixture was diluted with EtOAc and the organic layer was washed as follows: brine, HCl (2%), $NaHCO_3$ (satd), and brine. The combined organic layer was dried over $MgSO_4$, evaporated, and purified by column chromatography (silica gel, EtOAc/hexane) to yield **14** as a white solid (1.65 g, 97%). ^{1}H NMR (300 MHz, $CDCl_3$) δ: 2.23 (s, *Me*STol), 4.06–3.99 (m, 2H, H-6′, H-5), 4.38 (dd, 1H, J_1 = 9.9 Hz, J_2 = 5.7 Hz, H-3), 4.63 (dd, 1H, J_1 = 12 Hz, J_2 = 3 Hz, H-6), 4.85 (d, 1H, J = 9.9 Hz, H-1), 5.18 (dd, 1H, $J_1 = J_2$ = 9.9 Hz, H-2), 5.32 (dd, 1H, $J_1 = J_2$ = 9.9 Hz, H-4), 6.87 (d, 2H, J = 7.8 Hz, *ortho* to the methyl of STol), 7.33 (d, 2H, J = 8.1 Hz, *ortho* to the sulfur of STol), 7.58–7.41 (m, BzO), 8.10–7.99 (m, BzO). ^{13}C NMR (125 MHz, $CDCl_3$) δ: 20.7 (*Me*STol), 62.6, 65.8, 69.0, 70.2, 86.0 (C-1), 127.9, 128.0, 128.1, 128.7, 129.2, 129.4, 129.5, 129.7, 132.7, 133.1, 133.3. ESIMS *m*/*z* 646.2 (M+Na^+, $C_{34}H_{29}N_3O_7S$ requires 646.7).

4.2.2. Compound 16. To a powdered, flame dried 4 Å molecular sieves (500 mg) anhydrous acetonitrile (3 mL), was added followed by the addition of acceptor **15** (150 mg, 0.15 mmol) and donor **14** (140 mg, 0.224 mmol). After being stirred for 10 min at room temperature, the mixture was treated with NIS (50 mg, 0.225 mmol). After additional 5 min at room temperature, the mixture was cooled to −40 °C and TfOH (cat.) was added. Propagation of the reaction was monitored by TLC (EtOAc 50%, hexane 50%). The reaction was diluted with EtOAc, and filtered through Celite. After thorough washing of the Celite with EtOAc, the washes were combined and extracted with 10% $Na_2S_2O_3$, saturated (aq) $NaHCO_3$, brine, dried over $MgSO_4$ and concentrated. The crude was purified by flash chromatography to yield **16** (130 mg, 57%). ^{1}H NMR (500 MHz, $CDCl_3$) ring **I** δ: 3.46–3.50 (m, 3H, H-2, H-6, H-6′), 4.53 (ddd, 1H, $J_1 = J_2 = J_3$ = 10.0 Hz, H-5), 5.06 (dd, 1H, $J_1 = J_2$ = 10.0 Hz, H-4), 5.44 (dd, 1H, $J_1 = J_2$ = 10.0 Hz, H-3), 6.11 (d, 1H, J = 4.0 Hz, H-1); ring **II**: δ 1.71 (ddd, 1H, $J_1 = J_2 = J_3$ = 12.5 Hz, H-2ax), 2.35 (dt, 1H, J_1 = 12.5, J_2 = 4.5 Hz, H-2eq), 3.30–3.36 (m, 1H, H-4), 3.43–3.48 (m, 1H, H-1), 3.77 (dd, 1H, $J_1 = J_2$ = 9.0 Hz, H-5), 3.96 (t, 1H, $J_1 = J_2$ = 9.0 Hz, H-4), 5.00 (dd, 1H, $J_1 = J_2$ = 9.5 Hz, H-6); ring **III**: δ 3.58–3.60 (dd, 1H, J_1 = 3.0 Hz, J_2 = 11.5 Hz, H-5′), 4.13 (m, 1H, H-4), 4.15 (dd, 1H, J_1 = 3.0 Hz, J_2 = 11.5 Hz, H-5), 4.28 (dd, 1H, $J_1 = J_2$ = 5.0 Hz, H-3), 4.76 (dd, 1H, J_1 = 1.0 Hz, J_2 = 6.0 Hz, H-2), 5.19 (d, 1H, J = 1.0 Hz, H-1); ring **IV** δ: 3.16 (dd, 1H, J_1 = 1.5, J_2 = 2.0 Hz, H-2), 3.17 (m, 1H, H-6), 3.33 (m, 1H, H-6′), 3.57 (m, 1H, H-5), 4.46 (d, 1H, J = 1.5 Hz, H-1), 4.59 (m, 1H, H-4), 4.92 (br s, 1H, H-3); ring **V**: δ 4.02 (dd, 1H, $J_1 = J_2$ = 10.0 Hz, H-3), 4.06–4.09 (m, 1H, H-5), 4.57 (m, 2H, H-6, H-6′), 4.74 (d, 1H, J = 7.5 Hz, H-1), 5.40 (dd, 1H, J_1 = 7.5, J_2 = 10.0 Hz, H-2), 5.41 (dd, 1H, $J_1 = J_2$ = 10.0 Hz, H-4). ^{13}C NMR (125 MHz, CDCl3) δ: 20.4, 20.6, 20.6, 20.7, 20.8, 25.9 (C-2), 50.2 (C-6‴), 51.0 (C-6′), 56.3, 58.2, 58.9, 60.87, 63.6, 64.7, 65.3, 67.5 (C-5″), 68.5, 68.7, 69.7, 70.2, 70.7, 71.9, 72.0 (C-6⁗), 72.5, 72.9, 74.8, 75.4, 76.7, 77.0, 77.3, 80.0, 83.0, 96.4 (C-1′), 98.8 (C-1‴), 101.2 (C-1⁗), 107.8 (C-1″), 127.7, 127.8, 128.3, 128.5, 128.7, 129.5, 129.6, 129.9, 130.2, 133.1, 133.6, 134.3, 164.5, 164.9, 165.9, 168.3, 169.6, 170.0, 170.3. ESIMS *m*/*z* 1561.6 (M+K^+, $C_{62}H_{67}N_{21}O_{26}$ requires 1561.4).

4.2.3. Compound 3. Compound **16** (130 mg, 0.085 mmol) was dissolved in 33% solution of $MeNH_2$ in EtOH (30 mL) and the mixture was stirred at room temperature for 24 h. The reagent and the solvent were removed by evaporation. The residue was dissolved in THF (4 mL), added with 0.1 M NaOH (2 mL), and stirred at room temperature for 10 min after which PMe_3 (1 M solution in THF, 0.89 mL, 0.89 mmol) was added. Propagation of the reaction was monitored by TLC [CH_2Cl_2/MeOH/H_2O/$MeNH_2$ (33% solution in EtOH), 10:15:6:15], which indicated completion after 1.5 h. The reaction mixture was purified by flash chromatography on a short column of silica gel while the column was washed as follows: THF, EtOAc, MeOH/EtOAc (1:1), MeOH, and finally the product was eluted with $MeNH_2$ (33% solution in EtOH). The fractions containing the product were evaporated under vacuum, re-dissolved in water and evaporated again to afford the free amine product **3** (53.3 mg, 81%). The product was dissolved in water, the pH was adjusted to 6.8 by H_2SO_4 (0.01 M), and lyophilized to afford the sulfate salt of **3** (72.8 mg, containing 73.2% of the product **3** as free amine form) as a white foamy solid: ^{1}H NMR (500 MHz, D_2O, pH 4.2, adjusted by H_2SO_4 0.01 M) ring **I** δ: 3.10–3.17 (m, 1H, H-4), 3.30–3.64 (m, 3H, H-2, H-6, H-6′), 3.75–3.87 (m, 1H, H-3), 3.96 (td, 1H, J_1 = 3.0 Hz, J_2 = 8.5 Hz, H-5), 5.81 (d, 1H, J = 5.5 Hz, H-1); ring **II** δ: 1.60 (ddd, 1H, $J_1 = J_2 = J_3$ = 13.0 Hz, H-2ax), 2.20 (dt, 1H, J_1 = 13.0 Hz, J_2 = 4.0 Hz, H-2eq), 3.10–3.17 (m, 3H, H-1, H-3, H-4), 3.75–3.87 (m, 1H, H-5), 4.24–4.30 (m, 1H, H-6); ring **III** δ: 3.30–3.64

(m, 1H, H-5), 4.13–4.15 (m, 1H, H-4), 4.24–4.30 (m, 1H, H-5′), 4.41 (dd, 1H, J_1 = 4.5 Hz, J_2 = 1.0 Hz, H-2), 4.65–4.67 (m, 1H, H-3), 5.32 (d, 1H, J = 1.0 Hz, H-1); ring **IV** δ: 3.30–3.64 (m, 4H, H-2, H-4, H-6, H-6′), 4.24–4.30 (m, 2H, H-3, H-5), 5.19 (d, 1H, J = 1.0 Hz, H-1); ring **V** δ: 3.10–3.17 (m, 1H, H-3), 3.30–3.64 (m, 3H, H-2, H-4, H-6′), 3.75–3.87 (m, 2H, H-5, H-6), 4.53 (d, 1H, J = 8.0 Hz, H-1). ^{13}C NMR (125 MHz, $CDCl_3$) δ: 30.0 (C-2), 39.9 (C-6′, C-6‴), 48.2, 49.8, 50.4, 53.0, 57.0, 59.5 (C-5″), 65.9, 67.0, 67.4, 67.9 C-6⁗), 68.1, 68.4, 68.5, 68.7, 69.4, 69.6, 70.6, 72.1, 72.5, 73.5, 76.2, 79.2, 85.1, 94.7 (C-1′), 95.1 (C-1‴), 102.6 (C-1⁗), 110.2 (C-1″). ESIMS m/z 814.4 ($M+K^+$, $C_{29}H_{57}N_7O_{17}$ requires 814.7).

4.3. Antibacterial activity

The MIC values were determined using the double-microdilution method according to the National Committee for Clinical Laboratory Standards (NCCLS)[36] with two different starting concentrations of the tested compound (640 and 1024 μg/mL). All the experiments were performed in triplicates and analogous results were obtained in two to four different experiments. The Kirby-Bauer disk diffusion method was also used according to the NCCLS protocol.[36]

4.4. Purification and kinetic analysis of APH(3′)-IIIa

The plasmid pETSACG1 carrying the APH(3′)-IIIa gene (GenBank Accession No. V01547) was generously provided by Prof. A. Berghuis, McGill University. The protein was overexpressed in *E. coli* BL21(DE3) and purified using anionic column, as described previously .[32]

The phosphoryl transfer activity of was monitored by the pyruvate kinase/lactate dehydrogenase coupled assay.[37,38] The assay measures the rate of NADH absorbance decrease at 340 nm, which is proportional to the rate of steady-state ATP consumption. The oxidation of NADH was followed by continuously monitoring the absorbance at 340 nm using Ultrospec 2100 pro UV/visible spectrophotometer (Amersham Biosciences). A typical assay mixture contained 50 mM Tris–HCl buffer (pH 7.5), 40 mM KCl, 10 mM $MgCl_2$, 0.11 mg/mL NADH, 2.5 mM PEP, 1 mM ATP, 20 u/mL pyruvate kinase, 20 u/mL lactate dehydrogenase and varied concentrations of the aminoglycoside analog (1–350 μM). The mixture was preincubated at 37 °C for 5 min and the reaction was initiated by addition of purified APH(3′)-IIIa (10 μL of 0.072 U/mL stock solution). Values of K_m and k_{cat} were determined by non-linear regression analysis using the program GraFit 5.0.[39]

4.5. ^{31}P NMR experiments

All ^{1}H-decoupled and ^{1}H-coupled ^{31}P NMR experiments were recorded on a Bruker Avance™ 300 spectrometer at 121.5 MHz with 2 s repetition time. Chemical shifts are reported (in ppm) relative to external orthophosphoric acid (δ = 0.0) in D_2O. All time course experiments were performed continuously at 37 °C, using 5 mm high-resolution NMR tubes and at each time point the spectrum was acquired in 32 scans. The reactions were carried out in Tris–HCl buffer (50 mM), pD 7.1, containing aminoglycoside (44 mM), KCl (40 mM), $MgCl_2$ (10 mM), and ATP (132 mM) in a total volume of 0.5 mL D_2O. A 3-fold molar excess of ATP was added to ensure complete phosphorylation of the aminoglycosides. The reactions were initiated by rapid addition of 150 μL purified APH(3′)-IIIa (0.72 U/mL stock solution in 50 mM Tris–HCl buffer in D_2O, pD 7.1).

4.6. Molecular docking

The crystal structures used were the complexes of APH(3′)-IIIa with AMP-PNP (2.4 Å resolution; PDB Accession No. 1J7U), and the ternary complexes with ADP and either KanA (2.4 Å resolution; PDB Accession No. 1L8T), or NeoB (2.7 Å resolution; PDB accession number 1L8U). The conformation of residues 147–170 of APH(3′)-IIIa was shown to be different with or without the antibiotic substrates, but was essentially identical in the two ternary complexes structures. Therefore, for the docking experiments we used the higher resolution protein structure from the ADP · KanA complex as a starting template. The KanA ligand and solvent molecules were removed from the protein structure, hydrogen atoms were added and charges assigned using DS Modeling Visualizer within the DS Modeling 1.2 platform of Accelrys. Since the structures of the ADP molecules in the ternary complexes with ADP · KanA or ADP · NeoB were practically identical to the ADP part of AMP-PNP in its structure with APH(3′)-IIIa, the ADP in the ADP · KanA complex was modified to ATP by adding the γ-phosphate according to the AMP-PNP structure.

Flexible docking experiments were performed using the Accelrys DS LigandFit program.[40] The binding site was defined from the location of the NeoB molecule according to the APH(3′)-IIIa · ADP · NeoB structure, and the volume of the binding site was further expanded beyond the volume of bound NeoB by a layer of site points. The Dreiding/Gasteiger force field was employed for computing ligand–protein interaction during the flexible docking, and 20 poses were retained from each experiment. Flexible in situ minimization of the obtained ligand poses was done using the CHARMm force field, and the resulting poses were scored using the LigScore2 scoring function. The LigandFit settings were optimized and verified by redocking the NeoB and KanA molecules into the APH(3′)-IIIa · ATP structure.

Acknowledgments

We thank Dr. Albert M. Berghuis (McGill University) for kindly providing us with the plasmid pETSACG1. This research was supported by the Israel Science Foundation founded by the Israel Academy of Sciences and Humanities (grant no. 766/04), and in part by the L. and L. Richmond Fund for Promotion of Research at the Technion. V.B. acknowledges the financial Support

by the Center of Absorption in Science, the Ministry of Immigration Absorption and the Ministry of Science and Arts, Israel (Kamea Program).

References and notes

1. Gross, L. J. *Science* **1994**, *265*, 590.
2. Page, M. G. *Science* **1994**, *265*, 589.
3. Powers, J. H. *Curr. Opin. Infect. Dis.* **2003**, *16*, 547.
4. Kotra, L. P.; Haddad, J.; Mobashery, S. *Antimicrob. Agents Chemother.* **2000**, *44*, 3249.
5. Davis, B. D. *Microbiol. Rev.* **1987**, *51*, 341.
6. *Aminoglycoside Antibiotics*; Umezawa, H., Hooper, I. R., Eds.; Springer: New York, Heidelberg, 1982; Vol. 62, p 267.
7. Moazed, D.; Noller, H. F. *Nature* **1987**, *327*, 389.
8. Woodcock, J.; Moazed, D.; Cannon, M.; Davies, J.; Noller, H. F. *EMBO J.* **1991**, *10*, 3099.
9. Carter, A. P.; Clemons, W. M.; Brodersen, D. E.; Morgan-Warren, R. J.; Wimberly, B. T.; Ramakrishnan, V. *Nature* **2000**, *407*, 340.
10. Vicens, Q.; Westhof, E. *Biopolymers* **2003**, *70*, 42.
11. Walter, F.; Vicens, Q.; Westhof, E. *Curr. Opin. Chem. Biol.* **1999**, *3*, 694.
12. Wright, G. D.; Berghuis, A. M.; Mobashery, S. *Adv. Exp. Med. Biol.* **1998**, *456*, 27.
13. Fong, D. H.; Berghuis, A. M. *EMBO J.* **2002**, *21*, 2323.
14. Ye, X.-S.; Zhang, L.-H. *Curr. Med. Chem.* **2002**, 929.
15. Fridman, M.; Belakhov, V.; Yaron, S.; Baasov, T. *Org. Lett.* **2003**, *5*, 3575.
16. Fridman, M.; Belakhov, V.; Lee, L. V.; Liang, F. S.; Wong, C. H.; Baasov, T. *Angew. Chem., Int. Ed.* **2005**, *44*, 447.
17. Thompson, P. R.; Hughes, D. W.; Wright, G. D. *Biochemistry* **1996**, *35*, 8686.
18. Michael, K.; Wang, H.; Tor, Y. *Bioorg. Med. Chem.* **1999**, *7*, 1361.
19. Sucheck, S. J.; Wong, A. L.; Koeller, K. M.; Boehr, D. D.; Draker, K.-A.; Sears, P. S.; Wright, G. D.; Wong, C. H. *J. Am. Chem. Soc.* **2000**, *122*, 5230.
20. Han, M. J.; Yoo, K. S.; Kim, Y. H.; Chang, J. Y. *Tetrahedron Lett.* **2002**, *43*, 5597.
21. Hendrix, M.; Alper, P. B.; Priestly, E. S.; Wong, C.-H. *Angew. Chem., Int. Ed.* **1997**, *36*, 95.
22. Komiyama, M.; Yoshinari, K. *J. Org. Chem.* **1997**, *62*, 2155.
23. Tor, Y. *ChemBioChem* **2003**, *4*, 998.
24. Hachler, H.; Santanam, P.; Kayser, F. H. *Antimicrob. Agents Chemother.* **1996**, *40*, 1254.
25. Masuda, N.; Sakagawa, E.; Ohya, S.; Gotoh, N.; Tsujimoto, H.; Nishino, T. *Antimicrob. Agents Chemother.* **2000**, *44*, 2242.
26. Westbrock-Wadman, S.; Sherman, D. R.; Hickey, M. J.; Coulter, S. N.; Zhu, Y. Q.; Warrener, P.; Nguyen, L. Y.; Shawar, R. M.; Folger, K. R.; Stover, C. K. *Antimicrob. Agents Chemother.* **1999**, *43*, 2975.
27. Poole, K. *Antimicrob. Agents Chemother.* **2005**, *49*, 479.
28. Emerson, J.; Rosenfeld, M.; McNamara, S.; Ramsey, B.; Gibson, R. L. *Pediatr. Pulmonol.* **2002**, *34*, 91.
29. Fitzsimmons, S. C. *J. Pediatr.* **1993**, *122*, 1.
30. Cheer, S. M.; Waugh, J.; Noble, S. *Drugs* **2003**, *63*, 2501.
31. Rosenfeld, M.; Gibson, R.; McNamara, S.; Emerson, J.; McCoyd, K. S.; Shell, R.; Borowitz, D.; Konstan, M. W.; Retsch-Bogart, G.; Wilmott, R. W.; Burns, J. L.; Vicini, P.; Montgomery, A. B.; Ramsey, B. *J. Pediatr.* **2001**, *139*, 572.
32. McKay, G. A.; Thompson, P. R.; Wright, G. D. *Biochemistry* **1994**, *33*, 6936.
33. Burk, D. L.; Hon, W. C.; Leung, A. K.; Berghuis, A. M. *Biochemistry* **2001**, *40*, 8756.
34. Hon, W. C.; McKay, G. A.; Thompson, P. R.; Sweet, R. M.; Yang, D. S.; Wright, G. D.; Berghuis, A. M. *Cell* **1997**, *89*, 887.
35. Guo, J.; Frost, J. W. *J. Am. Chem. Soc.* **2002**, *124*, 10642.
36. National Committee for Clinical Laboratory Standards, Performance standards for antimicrobial susceptibility testing. Fifth information supplement: Approved Standard M100-S5. ed, NCCLS: Villanova, Pa., 1994.
37. Goldman, P. R.; Northrop, D. B. *Biochem. Biophys. Res. Commun.* **1976**, *69*, 230.
38. Perlin, M. H.; McCarty, S. C.; Greer, J. P. *Anal. Biochem.* **1988**, *171*, 145.
39. Leatherbarrow, R. J.; *GraFit 5.* ed.; Erithacus Software Ltd.: Horley, U.K., 2001.
40. Venkatachalam, C. M.; Jiang, X.; Oldfield, T.; Waldman, M. *J. Mol. Graphics. Modell.* **2003**, *21*, 289.